NANO LETTERS

pubs.acs.org/NanoLett

Letter

Ultrafast Laser Control of Antiferromagnetic–Ferrimagnetic Switching in Two-Dimensional Ferromagnetic Semiconductor Heterostructures

Zhaobo Zhou, Zhenfa Zheng, Junjie He, Jinlan Wang,* Oleg V. Prezhdo,* and Thomas Frauenheim*

Cite This: *Nano Lett.* 2023, 23, 5688–5695

Read Online

ACCESS | Metrics & More | Article Recommendations | Supporting Information

ABSTRACT: Realizing ultrafast control of magnetization switching is of crucial importance for information processing and recording technology. Here, we explore the laser-induced spin electron excitation and relaxation dynamics processes of $CrCl_3$/$CrBr_3$ heterostructures with antiparallel (AP) and parallel (P) systems. Although an ultrafast demagnetization of $CrCl_3$ and $CrBr_3$ layers occurs in both AP and P systems, the overall magnetic order of the heterostructure remains unchanged due to the laser-induced equivalent interlayer spin electron excitation. More crucially, the interlayer magnetic order switches from antiferromagnetic (AFM) to ferrimagnetic (FiM) in the AP system once the laser pulse disappears. The microscopic mechanism underpinning this magnetization switching is dominated by the asymmetrical interlayer charge transfer combined with a spin-flip, which breaks the interlayer AFM symmetry and ultimately results in an inequivalent shift in the moment between two FM layers. Our study opens up a new idea for ultrafast laser control of magnetization switching in two-dimensional opto-spintronic devices.

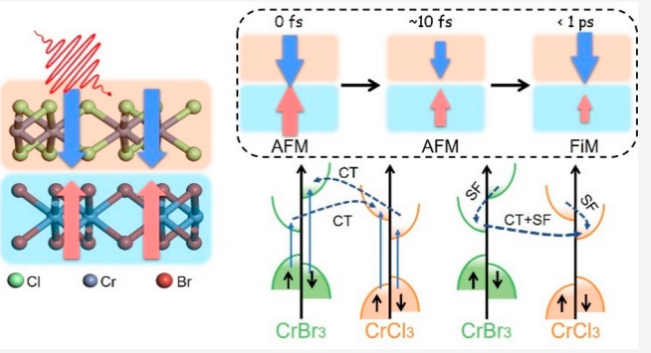

KEYWORDS: *two-dimensional ferromagnet, magnetization switching, ultrafast spin dynamics, time-dependent density functional theory, nonadiabatic molecular dynamics*

The ultrafast control of magnetization switching is a booming topic in spintronics since the speed of information storage and processing is determined by the fundamental time scales at which matter can be manipulated by external fields. Traditional strategies, e.g., gate voltage, magnetic field, and strain engineering,[1−6] which need to provide long-range external stimuli to change the exchange interactions between magnetic atoms in the ground state, are often sluggish and energy-consuming. Ultrafast laser pulses, however, are capable of controlling material magnetic order to switch the magnetization of devices at the picosecond to femtosecond time scales, revolutionizing information recording and processing by achieving the fastest and least-dissipative power possible.[7−11] Exploring laser control of magnetization switching and elucidating the underlying physics of this process in magnetic materials are thus of great importance for developing innovative opto-spintronics devices.

Since the first report of a magnetic order transition from antiferromagnetic (AFM) to ferromagnetic (FM) in FeRh thin films under a laser pulse excitation,[12] a series of important advances in magnetization switching of AFM alloys or layer stacks have been reported due to their ultrafast dynamics, insensitivity to external magnetic fields and absence of stray magnetic fields.[13−17] Several well-accepted origins and mechanisms, e.g., optical-induced phase transitions,[18] optical intersite spin transfer (OISTR) effect,[9,14] valley Zeeman effect,[19] and magnetic proximity effect (MPE),[20] have also been explored to gain a deeper understanding of these novel phenomena. Upon the coming of the post-Moore era, the recently discovered two-dimensional (2D) van der Waals (vdW) magnets, e.g., CrI_3,[21] Fe_3GeTe_2,[22] $Cr_2Ge_2Te_6$,[23] VSe_2,[24] $MnSe_2$,[25] and their derivative heterostructures,[26−29] provide a promising platform for controlling the magnetic behavior or spin-related phenomena in 2D limit using laser pulse due to their stable long-range magnetic order. Laser-induced spin injection, magnetic anisotropy, interfacial magnetic proximity coupling, and valley polarization in the 2D magnetic monolayer or heterointerface[26,30−32] are prominent examples of light-controlled magnetic properties in 2D magnets. Nonetheless, generating the transient FM state in 2D AFM

Received: April 12, 2023
Revised: June 6, 2023
Published: June 12, 2023

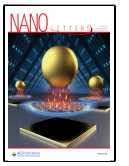

https://doi.org/10.1021/acs.nanolett.3c01350
Nano Lett. 2023, 23, 5688–5695

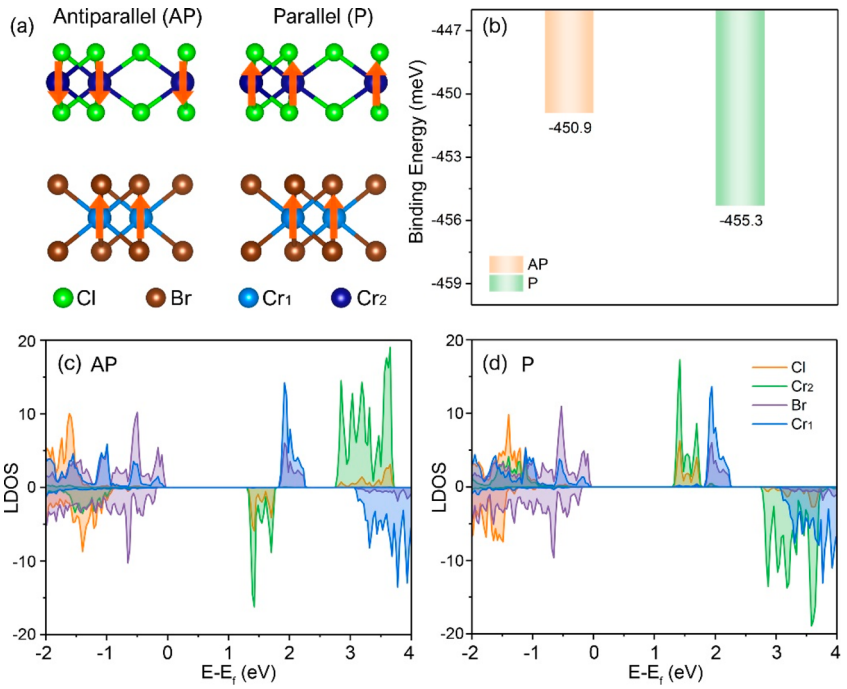

Figure 1. Ground state information on the $CrCl_3/CrBr_3$ heterostructures. (a) Spin configurations of the heterostructures. The orange arrows represent the direction of magnetic order of Cr atoms, forming the AP (left panel) and P (right panel) stacking systems. (b) Binding energy of the AP and P systems. The energy difference between these two systems is only 4.4 meV. (c,d) Local DOS for the AP and P systems. The band alignment is type-I for spin-up channel and type-II for spin-down channel respectively in the AP system. In contrast, they are type II for both spin-up and spin-down channels in the P system. The Fermi level is set to 0.

materials is relatively difficult and is less studied. The key technological challenge is to achieve efficient 180° magnetic order reversal on ultrafast time scales because it is hard to break the required time-reversal symmetry with the electric field of a laser pulse.

Beyond the FM state, the ferrimagnetic (FiM) state, which possesses inherent opposing magnetic moments of different magnitudes, offers technological advantages to solve this dilemma. Their easily controllable and detectable net magnetization, as well as high switching energy efficiency allow for small spin textures,[33] fast spin dynamics,[34,35] and ultrafast optical switching,[36,37] making them appealing candidates for ultrafast optical control of magnetization switching. Therefore, exploring an effective AFM-to-FiM switching and unveiling the basic physics in 2D magnets or vdW heterostructures is critical to realize practical application in 2D opto-spintronic devices.

In this work, by combining real-time time-dependent density functional theory (rt-TDDFT) and ab initio nonadiabatic molecular dynamics (NAMD) simulation, we systematically explore the laser-driven spin dynamics processes of $CrCl_3/CrBr_3$ heterostructures with antiparallel and parallel arrangements. Our simulations show that upon excitation by a laser pulse, ultrafast demagnetization of $CrCl_3$ and $CrBr_3$ layers will occur in two systems, but their magnetic order will be kept, which is attributed to laser-induced equivalent interlayer spin electron excitation. Following the dissipation of the laser pulse, photoexcited spin electrons relax via a nonequilibrium pathway, breaking the AFM symmetry and leading to interlayer AFM-to-FiM magnetization switching in the antiparallel arrangement. Such magnetization switching is mainly attributed to asymmetrical charge transfer and spin-flip from the spin-up channel of $CrBr_3$ to the spin-down channel of $CrCl_3$. Further analysis reveals that the SOC effect and optical out-of-plane A_{1g} phonon mode of the two layers significantly contributed to this dynamics process. Overall, this work demonstrates ultrafast laser control of an AFM-to-FiM switching in a 2D magnetic vdW heterostructure and provides new insights into the design of novel 2D opto-spintronic devices.

Before exploring the laser-induced spin dynamics processes, we should first investigate the ground state properties (see the computational details in the Supporting Information). Owing to the close lattice constants of two layers, the heterostructures are built by the unit cells with the most stable AB stacking configuration (Figure S1 and Table S1). Additionally, different ferromagnetic layers in heterostructures have different coercivities, as determined by the magnetic anisotropy energy (MAE). Thus, two spin configurations including antiparallel (AP) system and parallel (P) system, corresponding to the interlayer AFM state and FM state, respectively, are considered in our work (Figure 1a). The calculated binding energies show that the P system is more stable due to its lower binding energy (Figure 1b). Nevertheless, the previous study of the hysteresis loop revealed the reversible magnetic order for the $CrCl_3$ layer under a magnetic field of ~0.4 T, keeping the AFM state of the $CrBr_3/CrCl_3$ heterostructures. Besides, the MAE of the $CrCl_3$ (14 ueV/f.u.) monolayer is also much smaller than that of the $CrBr_3$ (129 ueV/f.u.) monolayer.[38] These results imply that the magnetization flip of the $CrCl_3$ layer can be accomplished under a small external magnetic field. Similar phenomena are also observed in the chromium trihalide bilayers in experiments.[21,39,40] Thus, although the P system shows higher stability in the ground state, the metastable AP system can still be achieved after a small steady magnetic field.

The local density of states (DOS) of spin-up and spin-down channels for the AP and P systems show that the valence band

https://doi.org/10.1021/acs.nanolett.3c01350
Nano Lett. 2023, 23, 5688−5695

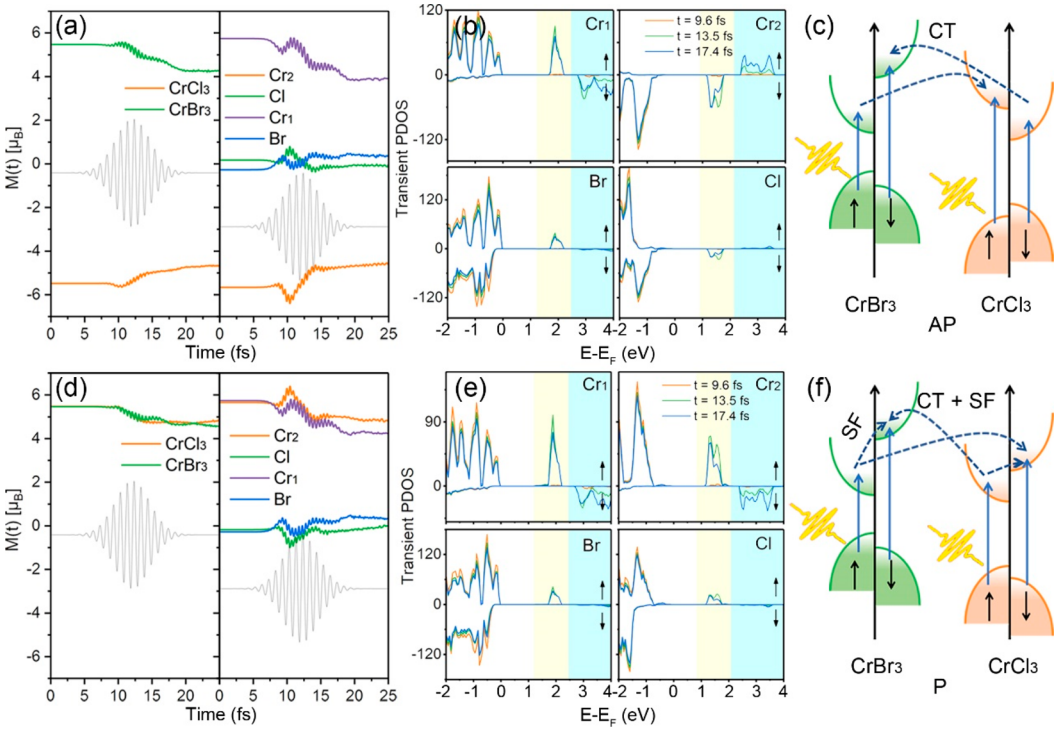

Figure 2. Ultrafast laser-induced spin dynamics of the $CrBr_3/CrCl_3$ heterostructures. (a, d) Time-dependent magnetic moment of each layer (left) and Cr, Cl, and Br atoms (right) for the AP and P systems, respectively. The gray oscillating line corresponds to the temporal profile of the vector potential of the laser pulse. (b, e) Time-dependent local DOS of the Cr_1, Cr_2, Br, and Cl atoms for the AP and P systems, respectively. Orange, green, and blue lines represent the transiently occupied DOS at t = 9.6, 13.5, and 17.4 fs, respectively. Black arrows pointing up and down indicate spin-up and spin-down channels, respectively. Yellow and cyan regions highlight the lower CB and higher CB, respectively. (c, f) Schematic diagram of laser-induced spin electron excitation processes for the AP and P systems. The spin electron is first excited from VB to CB in the two systems. Then, the spin electron will hop via the CT pathway in the AP system but not the CT+SF or SF pathway in the P system.

(VB) and conduction band (CB) are primarily contributed by Cl/Br atoms and Cr atoms, respectively (Figure 1c,d). This implies that electrons in the two spin channels tend to be first excited from nonmetal atoms to magnetic metal atoms and their magnetic moments could change simultaneously. Furthermore, the band alignment of the spin-up and spin-down channel in the AP system is type-I and type-II respectively, while in the P system they are both type-II. Such asymmetric band alignment will produce diverse spin electron relaxation pathways after the laser pulse excitation, and the total magnetic moment depends directly on the amount of difference between the electron in spin-up and spin-down channels. Herein, the spin-up (spin-down) channel of $CrBr_3$ lost (gain) electrons or the spin-up (spin-down) channel of $CrCl_3$ gained (lost) electrons will result in the demagnetization of the two layers in the AP system. In comparison, the spin-up (spin-down) channel of the two layers in the P system lost (gain) electron will induce demagnetization. Thus, the laser-induced spin electron dynamics processes of the $CrCl_3/CrBr_3$ heterostructures should be further investigated to assess the magnetic order switching.

We first excited two systems using an ultrafast laser pulse based on rt-TDDFT calculations (see the computational details in the Supporting Information). The calculated time-dependent total magnetic moments of the $CrCl_3$ and $CrBr_3$ layers decrease rapidly within ∼10 fs, revealing their ultrafast demagnetization process in both systems (left panel in Figure 2a,d). However, the magnetic order of each layer remains unchanged, and the demagnetization of two layers is also close (∼1.5 μ_B) in the two systems, suggesting that the AP and P systems still preserve the AFM and FM states, respectively, during the laser excitation, despite the ultrafast demagnetization occurring. Further analysis of the changes in the atomic magnetic moment reveals that the demagnetization mainly originates from the magnetic Cr atoms (right panel in Figure 2a,d). Simultaneously, the nonmagnetic Cl/Br atoms are magnetized and participate in the demagnetization process as well, as expected considering the MPE from the magnetic atoms.[20] In particular, the MPE of Cr atoms results in local magnetic moments of 0.16/−0.26 and −0.18/−0.28 μ_B for the Cl/Br atoms in the AP and P systems, respectively. The relatively higher magnetic moments of the Cr/Br atoms in the P system originate from the smaller interlayer distance (Figure S2), which decreases the distance between the Cl/Br atoms and the Cr atoms in the adjacent layer and enhances the interlayer MPE of the Cr atoms. Besides, the time-dependent magnetic moment of Cr atoms is opposite to that of Cl/Br atoms at the beginning of the demagnetization process (Figure S3), a signature of the OISTR effect,[14] highlighting the fact that the spin-polarized electron will transfer between Cr atoms and Cl/Br atoms in each layer before hopping to the neighboring FM layer.

To establish the OISTR mechanism of the two systems, we calculate their atomic transient local DOS at different times (Figure 2b,e). The DOS of the VB decreases over time, but for the CB, the situation becomes complex. The DOS of each atom increases initially and subsequently decreases at the lower CB (yellow region), whereas it increases steadily at the higher CB (cyan region) during the interval of 9.6−17.4 fs. These results demonstrate that the spin-polarized electron will be first

https://doi.org/10.1021/acs.nanolett.3c01350
Nano Lett. 2023, 23, 5688−5695

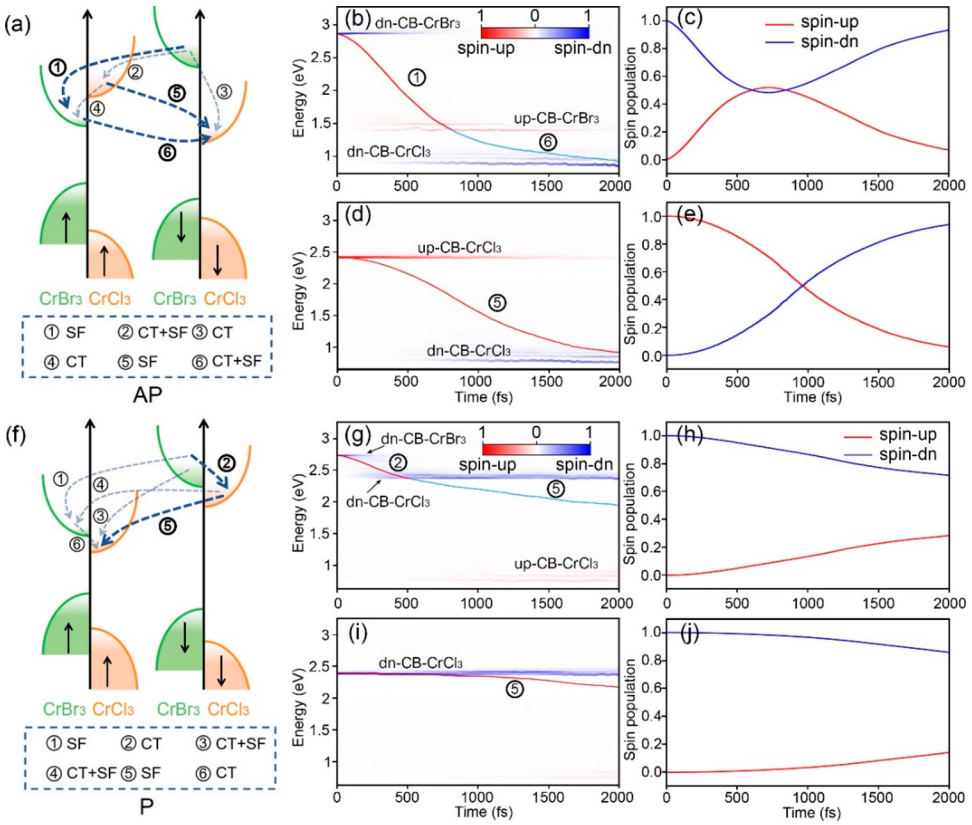

Figure 3. Spin electron relaxation dynamics of $CrCl_3/CrBr_3$ heterostructures from NAMD simulations (see the computational details in Supporting Information). (a, f) Schematic diagram of spin electron relaxation pathways in the AP and P systems, respectively. Bold dashed arrows represent the most probable dynamics pathway. Black arrows pointing up and down indicate spin-up and spin-down channels, respectively. Energy relaxation of excited spin electron for (b, d) the AP system and (g, i) P the system, where the color map indicates orbital localization. The up-CB-$CrBr_3$, dn-CB-$CrBr_3$, up-CB-$CrCl_3$ and dn-CB-$CrCl_3$ represent the energy level of spin-up CB of $CrBr_3$, spin-down CB of $CrBr_3$, spin-up CB of $CrCl_3$ and spin-down CB of $CrCl_3$, respectively. The red and cyan delay lines represent processes ① and ⑥ for the AP system and processes ② and ⑤ for the P system. Spin population of excited spin electron for (c, e) the AP system and (h, j) the P system. The red and blue lines represent the probability that spin electrons localize in the spin-up and spin-down channels, respectively.

excited from VB to CB in each layer and then transfer between two layers, leading to an equivalent change in the magnetic moment of the two FM layers. Such an indirect OISTR mainly involves two dynamics processes: intralayer excitation and interlayer transfer, as opposed to the direct OISTR in traditional magnetic-based metal heterojunctions (e.g., Co/Mn,[14,15] Co/Cu,[41] Ni/Pt,[9] and Ni/Mn).[42]

In addition to OISTR, spin−orbit coupling (SOC) also plays a key role in the demagnetization process of such magnets, as the spin-flip (SF) is allowed when the SOC term in the time-dependent Kohn−Sham equation is considered (eq S1).[41,43,44] Here, we calculate and compare the time-dependent magnetic moments of each atom with and without SOC for the AP and P system (Figure S4). We find that SOC has a significant effect on the atomic magnetic moment in the P system after 13.5 fs, but it can be ignored in the AP system. Accordingly, when the $CrCl_3/CrBr_3$ heterostructure is excited by the laser pulse, the ultrafast demagnetization of two FM layers in the AP system is mainly attributed to interlayer charge transfer (CT) of the same spin channel, and the SOC-induced SF will contribute to their demagnetization in the P system. Based on our analysis, we conclude that the spin electron dynamics of the $CrCl_3/CrBr_3$ heterostructures with the AP and P systems can be divided into two parts (Figure 2c and 2f): (1) laser-induced intralayer excitation of the spin-polarized electron and (2) pure CT for the AP system or mixed SF and CT for the P system. It should be noted that intralayer SF in the $CrCl_3$ and $CrBr_3$ layers may also occur in the P system. In this case, the spin electron will still reside in the higher spin-polarized CB of two FM layers for two systems ultimately. Therefore, our conclusion remains unchanged whether intralayer SF is considered or not.

The laser-induced spin electron excitation dynamics processes of the $CrCl_3/CrBr_3$ heterostructures were systematically explored. The total magnetic order remains AFM and FM for the AP and P systems, respectively. Once the laser is removed (>20 fs), the excited spin electron will relax from higher CB to lower CB and may affect the magnetic order of heterostructures, thus requiring further investigation. According to the band alignment of the spin-up and spin-down channels of the AP and P systems, the spin electron relaxation can be divided into six dynamics processes involving CT, SF, and CT+SF (Figure 3a,f). The time-dependent energy and spin relaxation of the excited electron by the spin-adiabatic representation in the two systems are shown in Figure 3b−e and Figure 3g−j, respectively. For the AP system, the photoexcited spin electron will first relax from the spin-down CB to the spin-up CB in $CrBr_3$ (process ①) and then transfer to the spin-down CB of $CrCl_3$ (process ⑥) with a time scale of 628 fs (Figure 3b), which is estimated by fitting with a Gaussian function. Such a relaxation process involves successive intralayer SF and interlayer CT+SF, leading to the

https://doi.org/10.1021/acs.nanolett.3c01350
Nano Lett. 2023, 23, 5688−5695

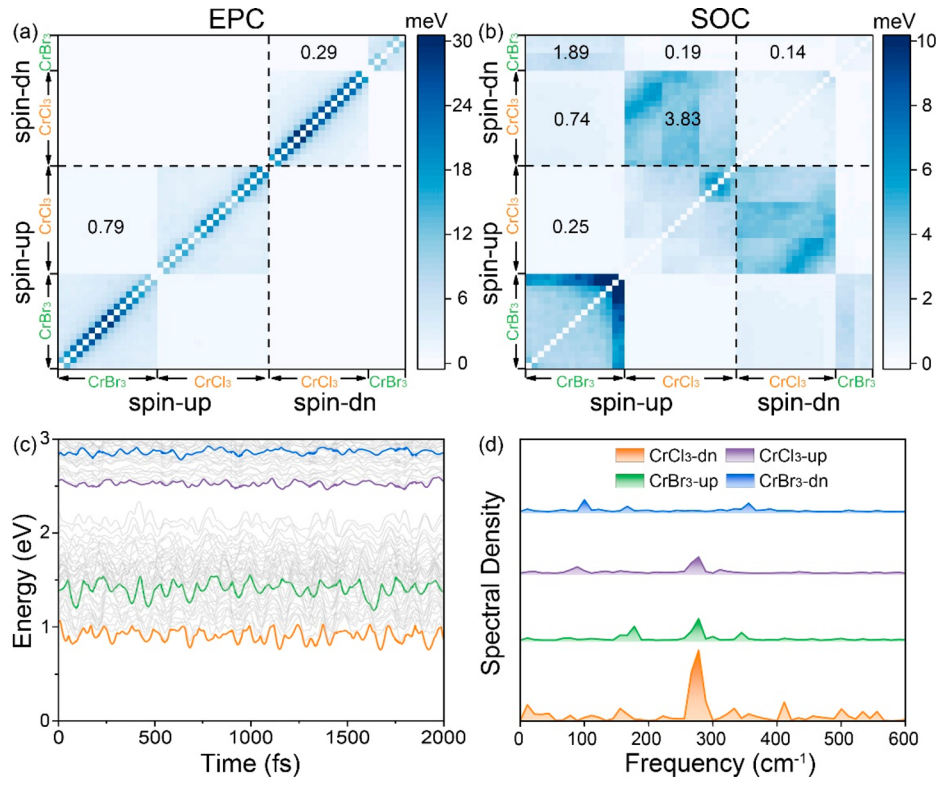

Figure 4. (a) EPC and (b) SOC between electronic states in the $CrCl_3/CrBr_3$ heterostructure in the AP system according to the spin-diabatic representation. The average NAC values between key states are listed. (c) Energy evolution of electronic states of CB at the Γ point and (d) Fourier transforms spectral densities of corresponding key states. The electronic structure, and in particular, electronic energy levels, are determined by the positions of atomic nuclei. Thus, variation of an energy level as a function of time is the consequence of fluctuations of atomic nuclei. Fourier transform on the variation of the energy level with respect to time reveals the coupling of the energy level to vibrational modes, allowing one to determine the dominant phonon frequencies.

initial increase and subsequent decrease of the spin-up electron population in $CrBr_3$ (Figure 3c). Meanwhile, the intralayer SF between the spin-up CB and spin-down CB in $CrCl_3$ occurs with a time scale of 755 fs (Figure 3d) and monotonically increases the spin-down electron population in $CrCl_3$ (Figure 3e). A distinct spin electron relaxation process occurs in the P system. It is found that the electron will first transfer between spin-down CBs from $CrBr_3$ to $CrCl_3$ (process ②), and then intralayer SF (process ⑤) occurs in the $CrCl_3$ layer within 5 ps (Figure 3g,i), as a result leading to the continued decrease of the spin-down electron population in $CrBr_3$ and increase of the spin-up electron population in $CrCl_3$ (Figure 3h,j).

Based on the NAMD calculations, we can give a clear description of the spin electron relaxation dynamics process (Figure S5). First, intralayer SF occurs in the $CrBr_3$ and $CrCl_3$ layers simultaneously within a subpicosecond time scale. In this case, the magnetic moments of the two layers will equivalently increase and maintain the interlayer AFM state. After that, the interlayer CT accompanied by SF between $CrBr_3$ and $CrCl_3$ reduces the magnetic moment of $CrBr_3$ but further increases the magnetic moment of $CrCl_3$. Such an inequivalent change in the magnetic moments breaks the interlayer AFM symmetry, thus leading to a magnetization switching from AFM to FiM in the AP system (Figure S6). Note that although the spin electron relaxation caused the change in the magnetic moments of the $CrCl_3$ and $CrBr_3$ layers in the P system, the direction of the magnetic order remains unchanged. Therefore, we conclude that the $CrCl_3/CrBr_3$ heterostructure with the P system will still retain the FM state during the whole spin dynamics process.

As of now, we have demonstrated effective interlayer AFM-to-FiM switching in the $CrCl_3/CrBr_3$ heterostructures with the AP system, thanks to the synergistic impact of CT+SF dynamics. To further uncover the factors contributing to such a dynamics process, we calculate the nonadiabatic coupling (NAC) matrix between different states using spin-diabatic representation.[45,46] The electron−phonon coupling (EPC) and SOC components are depicted in Figure 4a,b, respectively. First, the SOC component between the spin-up and spin-down states for $CrBr_3$ (1.89 meV) is larger than the EPC component between the spin-down states of $CrBr_3$ and spin-down states of $CrCl_3$ (0.29 meV). Meanwhile, the SOC component between spin-up states and spin-down states for $CrCl_3$ (3.83 meV) is larger than the EPC component between spin-up states of $CrCl_3$ and spin-up states of $CrBr_3$ (0.79 meV), explaining why the spin-down (spin-up) electron in the $CrBr_3$ ($CrCl_3$) layer prefers to first relax via the intralayer SF pathway (processes ① and ⑤), rather than to transfer between the two layers through the CT pathway. Similarly, the interlayer SF +CT (process ⑥), which is the only relaxation pathway, is mainly contributed by the SOC component, and the EPC component has no contribution due to their opposite spin states. Therefore, we conclude that the SOC effect plays an important role in determining the spin relaxation dynamics pathway.

Besides, the lattice thermal fluctuation, which can be assessed by comparing the frequencies of the phonon modes

https://doi.org/10.1021/acs.nanolett.3c01350
Nano Lett. 2023, 23, 5688−5695

participating in the spin electron relaxation dynamics, cannot be overlooked, as the spin electron relaxation dynamics occur on a subpicosecond time scale. During the electron relaxation process, the lattice thermal fluctuation can alter the electron environment due to lattice distortions, which affect the positions of the ions and their electronic properties. As a result, the SOC interaction can be further enhanced and trigger the SF pathway. To further understand the effect of lattice thermal fluctuation on the spin electron relaxation dynamics, the energy evolution of each CB level for the AP system and their Fourier transform spectra are depicted in Figures 4 and S7. We observed that the main peaks of each state with the same spin channel are similar, and four key Fourier transform spectra are thus taken as examples to illustrate the role of lattice fluctuation in the spin electron relaxation dynamics (Figure 4d). The dominant vibrational signals at 178.58 and 89.09 cm^{-1} can be assigned to the A_{1g} mode (185 cm^{-1}) and E_g mode (80 cm^{-1}) of $CrBr_3$, while the signals at 280.37, 99.25, and 350.10 cm^{-1} can be attributed to the A_{1g} (305.3 and 119.7 cm^{-1}) and E_g (351.7 cm^{-1}) modes of $CrCl_3$.[47] That is, the lattice fluctuation of the $CrCl_3$ layer primarily induced the intralayer SF dynamics, whereas the key interlayer CT+SF dynamics is driven by the lattice fluctuation of both $CrCl_3$ and $CrBr_3$ layers. Further visualization of the corresponding vibration vectors (Figure S8) suggests that the optical A_{1g} modes of $CrCl_3$ and $CrBr_3$ are the most important modes for interlayer CT+SF dynamics. By contrast, other phonon modes have little contribution to the spin electron relaxation and only induce time-dependent energy fluctuation of other donor states. Therefore, the excitation of the optical out-of-plane A_{1g} modes of the two FM layers will effectively participate in the magnetization switching of AFM-to-FiM.

In summary, we have performed rt-TDDFT and NAMD simulations to investigate the ultrafast laser-induced spin dynamics processes of 2D $CrCl_3/CrBr_3$ heterostructures involving AP and P systems. Our results show that laser pulse induces ultrafast demagnetization of two FM layers within 10 fs but still maintains their intrinsic AFM and FM state for the AP and P systems, respectively. Such phenomenon is primarily attributed to the laser-excited equivalent interlayer spin electron excitation. More importantly, the spin electron relaxation along the interlayer CT+SF pathway from spin-up channel of the $CrBr_3$ layer to spin-down channel of the $CrCl_3$ layer induces an inequivalent change in the magnetic moment of the two layers, breaks the symmetry of the interlayer AFM state and ultimately leads to a fast magnetization switching from the AFM to FiM state in the AP system within a subpicosecond time scale. Furthermore, NAC and phonon effect analysis reveals that the interlayer CT+SF dynamics process is mainly contributed by the optical out-of-plane A_{1g} phonon mode of the $CrCl_3$ layer, and the SOC effect cannot be overlooked. In light of these novel results, we suggest utilizing an ultrafast laser pulse to achieve AFM-to-FiM switching in 2D magnetic heterostructures with the interlayer AFM state, which will enable a practical application to high-speed 2D information storage devices and optical switching.

■ ASSOCIATED CONTENT

Supporting Information

The Supporting Information is available free of charge at https://pubs.acs.org/doi/10.1021/acs.nanolett.3c01350.

Computational details; stacking configurations, time-dependent atomic magnetic moment, schematic diagram of spin electron relaxation pathway for the AP and P systems; changes in the magnetic moment, Fourier transforms spectral densities, and the dominant vibration vectors for the AP system (PDF)

■ AUTHOR INFORMATION

Corresponding Authors

Thomas Frauenheim − *School of Science, Constructor University, Bremen 28759, Germany; Beijing Computational Science Research Center, Beijing 100193, China; Shenzhen JL Computational Science and Applied Research Institute, Shenzhen 518109, China*; Email: thomas.frauenheim@bccms.uni-bremen.de

Oleg V. Prezhdo − *Departments of Chemistry, and Physics and Astronomy, University of Southern California, Los Angeles, California 90089, United States*; orcid.org/0000-0002-5140-7500; Email: prezhdo@usc.edu

Jinlan Wang − *School of Physics, Southeast University, Nanjing 211189, China*; orcid.org/0000-0002-4529-874X; Email: jlwang@seu.edu.cn

Authors

Zhaobo Zhou − *Bremen Center for Computational Materials Science, University of Bremen, Bremen 28359, Germany*; orcid.org/0000-0003-2904-1845

Zhenfa Zheng − *Department of Physics, University of Science and Technology of China, Hefei, Anhui 230026, China*

Junjie He − *Department of Physical and Macromolecular Chemistry, Faculty of Science, Charles University in Prague, Prague 12843, Czech Republic*; orcid.org/0000-0001-6447-7893

Complete contact information is available at: https://pubs.acs.org/10.1021/acs.nanolett.3c01350

Notes

The authors declare no competing financial interest.

■ ACKNOWLEDGMENTS

This work was supported by the DFG Research and Training Group RTG 2247 "Quantum Mechanical Materials Modelling". J.W. was supported by the National Key Research and Development Program of China (grant 2021YFA1500703), the Natural Science Foundation of China (grants 22033002 and 92056112) and the Basic Research Program of Jiangsu Province (BK20222007). O.V.P. acknowledges support of the US National Science Foundation, grant CHE-2154367. The authors also thank the computational resources at the Supercomputer Center of Northern Germany via HLRN.

■ REFERENCES

(1) Ma, Y.; Dai, Y.; Guo, M.; Niu, C.; Zhu, Y.; Huang, B. Evidence of the Existence of Magnetism in Pristine VX_2 Monolayers (X = S, Se) and Their Strain-Induced Tunable Magnetic Properties. *ACS Nano* **2012**, *6*, 1695−1701.

(2) Burch, K. S. Electric switching of magnetism in 2D. *Nat. Nanotechnol.* **2018**, *13*, 532.

(3) Wang, Y.; Wang, C.; Liang, S.-J.; Ma, Z.; Xu, K.; Liu, X.; Zhang, L.; Admasu, A. S.; Cheong, S.-W.; Wang, L.; Chen, M.; Liu, Z.; Cheng, B.; Ji, W.; Miao, F. Strain-Sensitive Magnetization Reversal of a van der Waals Magnet. *Adv. Mater.* **2020**, *32*, 2004533.

(4) Lv, H.; Niu, Y.; Wu, X.; Yang, J. Electric-Field Tunable Magnetism in van der Waals Bilayers with A-Type Antiferromagnetic Order: Unipolar versus Bipolar Magnetic Semiconductor. *Nano Lett.* **2021**, *21*, 7050−7055.
(5) Li, D.; Li, S.; Zhong, C.; He, J. Tuning magnetism at the two-dimensional limit: a theoretical perspective. *Nanoscale* **2021**, *13*, 19812−19827.
(6) Huang, C.; Zhou, J.; Sun, H.; Wu, F.; Hou, Y.; Kan, E. Toward Room-Temperature Electrical Control of Magnetic Order in Multiferroic van der Waals Materials. *Nano Lett.* **2022**, *22*, 5191−5197.
(7) Stamm, C.; Kachel, T.; Pontius, N.; Mitzner, R.; Quast, T.; Holldack, K.; Khan, S.; Lupulescu, C.; Aziz, E. F.; Wietstruk, M.; Dürr, H. A.; Eberhardt, W. Femtosecond modification of electron localization and transfer of angular momentum in nickel. *Nat. Mater.* **2007**, *6*, 740−743.
(8) Rudolf, D.; La-O-Vorakiat, C.; Battiato, M.; Adam, R.; Shaw, J. M.; Turgut, E.; Maldonado, P.; Mathias, S.; Grychtol, P.; Nembach, H. T.; et al. Ultrafast magnetization enhancement in metallic multilayers driven by superdiffusive spin current. *Nat. Commun.* **2012**, *3*, 1037.
(9) Siegrist, F.; Gessner, J. A.; Ossiander, M.; Denker, C.; Chang, Y.-P.; Schröder, M. C.; Guggenmos, A.; Cui, Y.; Walowski, J.; Martens, U.; Dewhurst, J. K.; Kleineberg, U.; Münzenberg, M.; Sharma, S.; Schultze, M. Light-wave dynamic control of magnetism. *Nature* **2019**, *571*, 240−244.
(10) Dabrowski, M.; Scott, J. N.; Hendren, W. R.; Forbes, C. M.; Frisk, A.; Burn, D. M.; Newman, D. G.; Sait, C. R. J.; Keatley, P. S.; N'Diaye, A. T.; Hesjedal, T.; van der Laan, G.; Bowman, R. M.; Hicken, R. J. Transition Metal Synthetic Ferrimagnets: Tunable Media for All-Optical Switching Driven by Nanoscale Spin Current. *Nano Lett.* **2021**, *21*, 9210−9216.
(11) Yao, K.; Steinbach, F.; Borchert, M.; Schick, D.; Engel, D.; Bencivenga, F.; Mincigrucci, R.; Foglia, L.; Pedersoli, E.; De Angelis, D.; et al. All-Optical Switching on the Nanometer Scale Excited and Probed with Femtosecond Extreme Ultraviolet Pulses. *Nano Lett.* **2022**, *22*, 4452−4458.
(12) Ju, G.; Hohlfeld, J.; Bergman, B.; van de Veerdonk, R. J. M.; Mryasov, O. N.; Kim, J.-Y.; Wu, X.; Weller, D.; Koopmans, B. Ultrafast Generation of Ferromagnetic Order via a Laser-Induced Phase Transformation in FeRh Thin Films. *Phys. Rev. Lett.* **2004**, *93*, 197403.
(13) Radu, I.; Vahaplar, K.; Stamm, C.; Kachel, T.; Pontius, N.; Dürr, H. A.; Ostler, T. A.; Barker, J.; Evans, R. F. L.; Chantrell, R. W.; Tsukamoto, A.; Itoh, A.; Kirilyuk, A.; Rasing, T.; Kimel, A. V. Transient ferromagnetic-like state mediating ultrafast reversal of antiferromagnetically coupled spins. *Nature* **2011**, *472*, 205−208.
(14) Dewhurst, J. K.; Elliott, P.; Shallcross, S.; Gross, E. K. U.; Sharma, S. Laser-Induced Intersite Spin Transfer. *Nano Lett.* **2018**, *18*, 1842−1848.
(15) Golias, E.; Kumberg, I.; Gelen, I.; Thakur, S.; Gordes, J.; Hosseinifar, R.; Guillet, Q.; Dewhurst, J. K.; Sharma, S.; Schussler-Langeheine, C.; Pontius, N.; Kuch, W. Ultrafast Optically Induced Ferromagnetic State in an Elemental Antiferromagnet. *Phys. Rev. Lett.* **2021**, *126*, 107202.
(16) Afanasiev, D.; Hortensius, J. R.; Ivanov, B. A.; Sasani, A.; Bousquet, E.; Blanter, Y. M.; Mikhaylovskiy, R. V.; Kimel, A. V.; Caviglia, A. D. Ultrafast control of magnetic interactions via light-driven phonons. *Nat. Mater.* **2021**, *20*, 607−611.
(17) Kašpar, Z.; Surýnek, M.; Zubáč, J.; Krizek, F.; Novák, V.; Campion, R. P.; Wörnle, M. S.; Gambardella, P.; Marti, X.; Němec, P.; Edmonds, K. W.; Reimers, S.; Amin, O. J.; Maccherozzi, F.; Dhesi, S. S.; Wadley, P.; Wunderlich, J.; Olejník, K.; Jungwirth, T. Quenching of an antiferromagnet into high resistivity states using electrical or ultrashort optical pulses. *Nat. Electron.* **2021**, *4*, 30−37.
(18) Rini, M.; Tobey, R. a.; Dean, N.; Itatani, J.; Tomioka, Y.; Tokura, Y.; Schoenlein, R. W.; Cavalleri, A. Control of the electronic phase of a Manganite by mode-selective vibrational excitation. *Nature* **2007**, *449*, 72−74.
(19) Li, W.; Lu, X.; Wu, J.; Srivastava, A. Optical control of the valley Zeeman effect through many-exciton interactions. *Nat. Nanotechnol.* **2021**, *16*, 148−152.
(20) He, J.; Li, S.; Bandyopadhyay, A.; Frauenheim, T. Unravelling Photoinduced Interlayer Spin Transfer Dynamics in Two-Dimensional Nonmagnetic-Ferromagnetic van der Waals Heterostructures. *Nano Lett.* **2021**, *21*, 3237−3244.
(21) Huang, B.; Clark, G.; Navarro-Moratalla, E.; Klein, D. R.; Cheng, R.; Seyler, K. L.; Zhong, D.; Schmidgall, E.; McGuire, M. A.; Cobden, D. H.; Yao, W.; Xiao, D.; Jarillo-Herrero, P.; Xu, X. Layer-dependent ferromagnetism in a van der Waals crystal down to the monolayer limit. *Nature* **2017**, *546*, 270−273.
(22) Deng, Y.; Yu, Y.; Song, Y.; Zhang, J.; Wang, N. Z.; Sun, Z.; Yi, Y.; Wu, Y. Z.; Wu, S.; Zhu, J.; Wang, J.; Chen, X. H.; Zhang, Y. Gate-tunable room-temperature ferromagnetism in two-dimensional Fe_3GeTe_2. *Nature* **2018**, *563*, 94−99.
(23) Gong, C.; Li, L.; Li, Z.; Ji, H.; Stern, A.; Xia, Y.; Cao, T.; Bao, W.; Wang, C.; Wang, Y.; Qiu, Z. Q.; Cava, R. J.; Louie, S. G.; Xia, J.; Zhang, X. Discovery of intrinsic ferromagnetism in two-dimensional van der Waals crystals. *Nature* **2017**, *546*, 265−269.
(24) Bonilla, M.; Kolekar, S.; Ma, Y.; Diaz, H. C.; Kalappattil, V.; Das, R.; Eggers, T.; Gutierrez, H. R.; Phan, M.-H.; Batzill, M. Strong room-temperature ferromagnetism in VSe_2 monolayers on van der Waals substrates. *Nat. Nanotechnol.* **2018**, *13*, 289−293.
(25) O'Hara, D. J.; Zhu, T.; Trout, A. H.; Ahmed, A. S.; Luo, Y. K.; Lee, C. H.; Brenner, M. R.; Rajan, S.; Gupta, J. A.; McComb, D. W.; Kawakami, R. K. Room Temperature Intrinsic Ferromagnetism in Epitaxial Manganese Selenide Films in the Monolayer Limit. *Nano Lett.* **2018**, *18*, 3125−3131.
(26) Seyler, K. L.; Zhong, D.; Huang, B.; Linpeng, X.; Wilson, N. P.; Taniguchi, T.; Watanabe, K.; Yao, W.; Xiao, D.; McGuire, M. A.; Fu, K. C.; Xu, X. Valley Manipulation by Optically Tuning the Magnetic Proximity Effect in WSe_2/CrI_3 Heterostructures. *Nano Lett.* **2018**, *18*, 3823−3828.
(27) Zhou, Z.; Zhang, X.; Guo, Y.; Zhang, Y.; Niu, X.; Ma, L.; Wang, J. Ultralong lifetime for fully photogenerated spin-polarized current in two-dimensional ferromagnetic/nonmagnetic semiconductor heterostructures. *Phys. Rev. B* **2021**, *103*, 245411.
(28) Wu, Y.; Zhang, S.; Zhang, J.; Wang, W.; Zhu, Y. L.; Hu, J.; Yin, G.; Wong, K.; Fang, C.; Wan, C.; et al. Néel-type skyrmion in WTe_2/Fe_3GeTe_2 van der Waals heterostructure. *Nat. Commun.* **2020**, *11*, 3860.
(29) Albarakati, S.; Tan, C.; Chen, Z. J.; Partridge, J. G.; Zheng, G.; Farrar, L.; Mayes, E. L. H.; Field, M. R.; Lee, C.; Wang, Y.; et al. Antisymmetric magnetoresistance in van der Waals Fe_3GeTe_2/graphite/Fe_3GeTe_2 trilayer heterostructures. *Sci. Adv.* **2019**, *5*, No. eaaw0409.
(30) Li, S.; Zhou, L.; Frauenheim, T.; He, J. Light-Controlled Ultrafast Magnetic State Transition in Antiferromagnetic-Ferromagnetic van der Waals Heterostructures. *J. Phys. Chem. Lett.* **2022**, *13*, 6223−6229.
(31) He, J.; Li, S.; Zhou, L.; Frauenheim, T. Ultrafast Light-Induced Ferromagnetic State in Transition Metal Dichalcogenides Monolayers. *J. Phys. Chem. Lett.* **2022**, *13*, 2765−2771.
(32) Kim, J.; Kim, K.-W.; Kim, B.; Kang, C.-J.; Shin, D.; Lee, S.-H.; Min, B.-C.; Park, N. Exploitable Magnetic Anisotropy of the Two-Dimensional Magnet CrI_3. *Nano Lett.* **2020**, *20*, 929−935.
(33) Caretta, L.; Mann, M.; Büttner, F.; Ueda, K.; Pfau, B.; Günther, C. M.; Hessing, P.; Churikova, A.; Klose, C.; Schneider, M.; Engel, D.; Marcus, C.; Bono, D.; Bagschik, K.; Eisebitt, S.; Beach, G. S. D. Fast current-driven domain walls and small skyrmions in a compensated ferrimagnet. *Nat. Nanotechnol.* **2018**, *13*, 1154−1160.
(34) Kim, K.-J.; Kim, S. K.; Hirata, Y.; Oh, S.-H.; Tono, T.; Kim, D.-H.; Okuno, T.; Ham, W. S.; Kim, S.; Go, G.; Tserkovnyak, Y.; Tsukamoto, A.; Moriyama, T.; Lee, K.-J.; Ono, T. Fast domain wall motion in the vicinity of the angular momentum compensation temperature of ferrimagnets. *Nat. Mater.* **2017**, *16*, 1187−1192.
(35) Cai, K.; Zhu, Z.; Lee, J. M.; Mishra, R.; Ren, L.; Pollard, S. D.; He, P.; Liang, G.; Teo, K. L.; Yang, H. Ultrafast and energy-efficient

https://doi.org/10.1021/acs.nanolett.3c01350
Nano Lett. 2023, 23, 5688−5695

spin-orbit torque switching in compensated ferrimagnets. *Nat. Electron.* **2020**, *3*, 37−42.
(36) Davies, C. S.; Janssen, T.; Mentink, J. H.; Tsukamoto, A.; Kimel, A. V.; van der Meer, A. F. G.; Stupakiewicz, A.; Kirilyuk, A. Pathways for Single-Shot All-Optical Switching of Magnetization in Ferrimagnets. *Phys. Rev. Appl.* **2020**, *13*, 024064.
(37) Kim, S. K.; Beach, G. S. D.; Lee, K. J.; Ono, T.; Rasing, T.; Yang, H. Ferrimagnetic spintronics. *Nat. Mater.* **2022**, *21*, 24−34.
(38) Guo, Y.; Zhang, Y.; Zhou, Z.; Zhang, X.; Wang, B.; Yuan, S.; Dong, S.; Wang, J. Spin-constrained optoelectronic functionality in two-dimensional ferromagnetic semiconductor heterojunctions. *Mater. Horiz.* **2021**, *8*, 1323−1333.
(39) Cai, X.; Song, T.; Wilson, N. P.; Clark, G.; He, M.; Zhang, X.; Taniguchi, T.; Watanabe, K.; Yao, W.; Xiao, D.; McGuire, M. A.; Cobden, D. H.; Xu, X. Atomically Thin $CrCl_3$: An In-Plane Layered Antiferromagnetic Insulator. *Nano Lett.* **2019**, *19*, 3993−3998.
(40) Zhang, Z.; Shang, J.; Jiang, C.; Rasmita, A.; Gao, W.; Yu, T. Direct Photoluminescence Probing of Ferromagnetism in Monolayer Two-Dimensional $CrBr_3$. *Nano Lett.* **2019**, *19*, 3138−3142.
(41) Chen, J.; Bovensiepen, U.; Eschenlohr, A.; Muller, T.; Elliott, P.; Gross, E. K. U.; Dewhurst, J. K.; Sharma, S. Competing Spin Transfer and Dissipation at Co/Cu(001) Interfaces on Femtosecond Timescales. *Phys. Rev. Lett.* **2019**, *122*, 067202.
(42) Elliott, P.; Muller, T.; Dewhurst, J. K.; Sharma, S.; Gross, E. K. Ultrafast laser induced local magnetization dynamics in Heusler compounds. *Sci. Rep.* **2016**, *6*, 38911.
(43) Dewhurst, J. K.; Shallcross, S.; Gross, E. K. U.; Sharma, S. Substrate-Controlled Ultrafast Spin Injection and Demagnetization. *Phys. Rev. Appl.* **2018**, *10*, 044065.
(44) Krieger, K.; Dewhurst, J. K.; Elliott, P.; Sharma, S.; Gross, E. K. Laser-induced demagnetization at ultrashort time scales: predictions of TDDFT. *J. Chem. Theory Comput.* **2015**, *11*, 4870−4874.
(45) Zheng, Z.; Zheng, Q.; Zhao, J. Spin-orbit coupling induced demagnetization in Ni: Ab initio nonadiabatic molecular dynamics perspective. *Phys. Rev. B* **2022**, *105*, 085142.
(46) Lei, Y.; Zheng, Z.; Vasquez, L.; Zhao, J.; Ma, J.; Ma, H. Enhanced Electron Transfer and Spin Flip through Spin-Orbital Couplings in Organic/Inorganic Heterojunctions: A Nonadiabatic Surface Hopping Simulation. *J. Phys. Chem. Lett.* **2022**, *13*, 4840−4848.
(47) Bermudez, V. M. Unit-Cell Vibrational-Spectra of Chromium Trichloride and Chromium Tribromide. *Solid State Commun.* **1976**, *19*, 693−697.

https://doi.org/10.1021/acs.nanolett.3c01350
Nano Lett. 2023, 23, 5688−5695